

# Radiofrequency Field-Induced Thermal Cytotoxicity in Cancer Cells Treated With Fluorescent Nanoparticles

Evan S. Glazer, MD<sup>1</sup> and Steven A. Curley, MD<sup>1,2</sup>

**BACKGROUND:** Nonionizing radiation, such as radiofrequency field and near infrared laser, induces thermal cytotoxicity in cancer cells treated with gold nanoparticles. Quantum dots are fluorescent semiconducting nanoparticles that were hypothesized to induce similar injury after radiofrequency field irradiation. **METHODS:** Gold nanoparticles and 2 types of quantum dot (cadmium-selenide and indium-gallium-phosphide) conjugated to cetuximab (C225), a monoclonal antibody against human epidermal growth factor receptor (EGFR)-1, demonstrated concentration-dependent heating in a radiofrequency field. The authors investigated the effect of radiofrequency field exposure after targeted nanoparticle treatment in a coculture of 2 human cancer cell lines that have differential EGFR-1 expression (a high-expressing pancreatic carcinoma, Panc-1, and a low-expressing breast carcinoma, Cama-1). **RESULTS:** Radiofrequency revealed that Panc-1 or Cama-1 cells not containing gold nanoparticles or quantum dots had a viability of >92%. The viability of Panc-1 cells exposed to the radiofrequency field after treatment with 50 nM Au-C225 was  $39.4\% \pm 8.3\%$  without injury to bystander Cama-1 cells (viability was  $93.7\% \pm 1.0\%$ ;  $P \sim .0006$ ). Panc-1 cells treated with targeted cadmium-selenide quantum dots were only 47.5% viable after radiofrequency field exposure ( $P < .0001$  compared with radiofrequency only Panc-1 control cells). Targeted indium-gallium-phosphide quantum dots decreased Panc-1 viability to  $58.2\% \pm 3.4\%$  after radiofrequency field exposure ( $P = \sim .0004$  compared with Cama-1 and Panc-1 controls). **CONCLUSIONS:** The authors selectively induced radiofrequency field cytotoxicity in Panc-1 cells without injury to bystander Cama-1 cells using EGFR-1-targeted nanoparticles, and demonstrated an interesting bifunctionality of fluorescent nanoparticles as agents for both cancer cell imaging and treatment. *Cancer* 2010;000:000-000. © 2010 American Cancer Society.

**KEYWORDS:** quantum dot, nanoparticle, noninvasive radiofrequency field treatment, photothermal therapy, hyperthermic cytotoxicity.

**Nanoparticle** based photodynamic therapy for cancer has been primarily focused on near-infrared radiation, because many nanoparticles absorb and release heat at these wavelengths.<sup>1,2</sup> These therapies are limited to superficial lesions, as near-infrared radiation transmission through tissue is minimal.<sup>3</sup> Other forms of electromagnetic radiation, including nonionizing radiofrequency field radiation, penetrates through biologic tissues readily and without significant toxicity.<sup>4</sup>

We have previously reported on the use of noninvasive radiofrequency fields to induce thermal cytotoxicity in human and mammalian cancer cells exposed to targeted solid gold nanoparticles and carbon nanotubes.<sup>5,6</sup> Cancer cells endocytose cell surface receptor-specific antibody-conjugated nanoparticles with subsequent intracellular heat release during shortwave radiofrequency field treatment sufficient to produce cellular cytotoxicity.<sup>5</sup> The radiofrequency treatment device consists of a transmitting plate connected to a radiofrequency power generator with a second grounded plate that together capacitively couple samples in a focused radiofrequency field. Gold nanoparticles heat in a concentration- and size-dependent linear fashion in this radiofrequency field.<sup>7</sup>

**Corresponding author:** Steven A. Curley, MD, Department of Surgical Oncology, Unit 444, The University of Texas M. D. Anderson Cancer Center, 1515 Holcombe Boulevard, Houston, TX 77030; Fax: (713) 745-5235; scurley@mdanderson.org

<sup>1</sup>Department of Surgical Oncology, The University of Texas M. D. Anderson Cancer Center, Houston, Texas; <sup>2</sup>Department of Mechanical Engineering and Materials Science, Rice University, Houston, Texas

We thank Dr. Paul Cherukuri for assistance in discussion of nanoparticle properties, and Kristine Ash, Kathryn Massey, and Katrina Briggs for administrative assistance and cell culture assistance.

**DOI:** 10.1002/cncr.25135, **Received:** September 22, 2009; **Accepted:** November 3, 2009, **Published online** in Wiley InterScience (www.interscience.wiley.com)

Theranostic nanoparticles, such as fluorescent nanocrystals (ie, quantum dots), are a category of nanoparticles that are fundamentally changing the way cancer is detected and treated.<sup>8</sup> Such nanoparticles can be targeted to malignant cells via antibody or peptide conjugation and can be used for optical imaging or as a marker for other therapeutic cargo.<sup>9-11</sup> Quantum dots in the far red region of the visible spectrum permit visualization of *in vivo* targets.<sup>12</sup> Typically, quantum dots consist of a metal core (~5 nm diameter) with an inorganic shell to improve quantum yield.<sup>13,14</sup> Common components of these cores include cadmium-selenide (CdSe) or indium-gallium-phosphide (InGaP). Polyethylene glycol (PEG), other polymers, proteins, or chemical hydroxylation are often used to prolong circulating time *in vivo* and to decrease potentially toxic metal ion release (ie, cadmium).<sup>15-18</sup>

In this work, we investigated an *in vitro* model of mixed cell populations to determine whether targeting selected cells with antibody-conjugated quantum dots or 20-nm gold nanoparticles followed by radiofrequency field treatment would kill the targeted cancer cells without injuring bystander cells. Human Panc-1 cells, a pancreatic carcinoma cell line, overexpresses epidermal growth factor receptor (EGFR)-1 that can be targeted with cetuximab (C225), a monoclonal antibody raised against this cell surface receptor. A human breast carcinoma cell line, Cama-1, minimally expresses EGFR-1,<sup>5</sup> and it represents the bystander or nontargeted cells.

We hypothesized that 1) like gold nanoparticles, quantum dots would heat in a 13.56-MHz radiofrequency field; and 2) targeting nanoparticles (gold or quantum dots) to cancer cells would result in thermal injury or death to targeted cells after radiofrequency field treatment without substantial effect on bystander cells.

## MATERIALS AND METHODS

### ***Cell Lines, Cell Culture, Antibodies, Quantum Dots, Gold Nanoparticles, and Fluorophores***

Cell lines Panc-1 and Cama-1 were purchased from American Type Culture Collection (Manassas, Va) and incubated in standard growth conditions (37°C, 5% CO<sub>2</sub>). During the experiment, all cultures were maintained in Dulbecco's Modified Eagle's Medium (Mediatech, Inc., Manassas, Va) supplemented with 10% fetal bovine serum and 1% penicillin/streptomycin. Experiments were performed in standard 60-mm culture dishes or 96-well plates (Corning Inc., Corning, NY). The cell line identities were confirmed by the Characterized Cell

Line Core service (STR DNA fingerprinting, The University of Texas M. D. Anderson Cancer Center, Houston, Tex, April 2009). Trypsin-ethylenediaminetetraacetic acid (EDTA; Mediatech) released cells from the cell culture dishes; 0.5 mg/mL collagenase I (Invitrogen Corp., Carlsbad, Calif) was added to the trypsin-EDTA solution to free cells from the 96-well plates.

Cetuximab (C225) was purchased from Bristol-Myers Squibb (New York, NY). Twenty-nanometer spherical gold nanoparticles were purchased from Ted Pella, Inc. (Redding, Calif). Antibody conjugation kits for CdSe-based quantum dots Qdot605 and Qdot705, and the fluorophore Alexa Fluor 647 were purchased from Invitrogen (Carlsbad, Calif). The InGaP-based quantum dot eFluor NC700 was purchased from eBioscience, Inc. (San Diego, Calif). CdSe-based quantum dots Qdot605 and Qdot705 emit peak fluorescence at ~605 nm and 705 nm, respectively.<sup>13</sup> InGaP eFluor NC700 quantum dots emit peak fluorescence at ~680 nm.<sup>19</sup> All contain a zinc-sulfide shell and PEG coating with a final hydrodynamic diameter of ~20 nm, similar to the gold nanoparticles used.<sup>20,21</sup> Quantum dots act as both the identification and therapeutic agent, and a fluorophore (Alexa Fluor 647) conjugated to C225 acted as the identifying fluorescent agent for all gold nanoparticle experiments.

All standard laboratory chemicals, including those required for antibody conjugation per instructions in each kit, were purchased from Sigma-Aldrich Corp. (St. Louis, Mo) or Thermo Fisher Scientific, Inc. (Waltham, Mass) unless otherwise stated.

### ***Conjugation of Cetuximab to Quantum Dots and Gold Nanoparticles***

Cetuximab was conjugated to Qdot605, Qdot705, and eFluor NC700 nanoparticles according to the manufacturer's instructions (noted above). Antibody-quantum dot conjugate concentrations were determined as recommended by measuring the absorbance with a Nanodrop spectrophotometer (Thermo-Fisher Scientific). Finally, the conjugates were sterilized under ultraviolet light for 15 minutes, a duration not reported to induce significant release of cytotoxic agents.<sup>22</sup>

Alexa Fluor 647 was conjugated to cetuximab also according to the manufacturer's instructions (noted above), and that conjugate (C225-Alexa Fluor 647) was subsequently conjugated to 20-nm gold nanoparticles with a slight modification to a previously published protocol.<sup>23</sup> First, the pH of gold nanoparticles stock solution was raised to approximately 8.5, the isoelectric point of cetuximab.<sup>24</sup> Next, 90 µg of C225-Alexa Fluor 647 was slowly added to

10 mL of the modified gold nanoparticles solution. This was protected from light to prevent fluorophore bleaching while gently mixing every 15 minutes at room temperature for 1 hour. Next, it was concentrated 10-fold in a centrifugation filter unit with a 100,000 molecular weight cutoff (Millipore Corp., Billerica, Mass) at 3500 g. Finally, it was sterilized under ultraviolet light for 15 minutes.

### **Generation of Radiofrequency Field and Antibody-Nanoparticle Conjugate Heating**

Samples were placed in a high-voltage, shortwave radiofrequency field (13.56 MHz) produced between 2 metal electrode plates that capacitively couple the sample plate in an air gap of 10 cm (Therm Med, LLC, Erie, PA). The radiofrequency field is on the order of 10 to 15 kV/m at 400 to 800 W of power.<sup>7</sup> Teflon, a material with low radiofrequency field absorbance, is used to hold samples in place. Stock solutions of each nanoparticle were diluted with 18 M $\Omega$  water to determine heating rates (Millipore).

Cells were exposed to the radiofrequency field for 5 minutes at a generator power of 200 W or for 4 minutes at 250 W as indicated (total energy generated,  $\sim$ 1000 W-minutes or 60 kJ). The temperature was continuously monitored with an infrared camera (FLIR Systems, Inc., Boston, Mass). All media temperatures remained  $<40.5^{\circ}\text{C}$ .

### **Panc-1 Cells Treated With Qdot605-Cetuximab and Radiofrequency Field Exposure**

An aliquot of Panc-1 cells were exposed to 50 nM Qdot605-cetuximab for 3 hours, and a separate aliquot of Panc-1 cells were exposed to an equal concentration of cetuximab only. After exposure, the cells were washed, combined in equal numbers ( $2 \times 10^5$  cells each) in cell culture dishes ( $n = 8$ ), and incubated for 24 hours. At that time, half of the dishes were exposed to a radiofrequency field for 5 minutes at a generator power of 200 W ( $n = 4$ ). Another group of combined cells ( $n = 4$ ) were not exposed to radiofrequency field treatment. Investigation of viability occurred 48 hours later with flow cytometry.

### **Mixed Cell Populations Treated With Cetuximab-Conjugated Nanoparticles and Subsequently Exposed to A Radiofrequency Field**

An equal number of Panc-1 and Cama-1 cells ( $3 \times 10^5$ ) were plated together in standard 60-mm cell culture dishes ( $n = 4$ ). After 24 hours, the cells were treated with 50 nM gold nanoparticles-C225-Alexa Fluor 647 for 3 hours. At the same time, an equal number of Panc-1 and

Cama-1 cells ( $2 \times 10^4$ ) were plated together in 96-well plates (replicates of 4). The cells in plates were treated with 50 nM eFluor NC700-C225 or 50 nM Qdot705-C225 for 3 hours. After treatment, the media was exchanged for fresh complete media without conjugates. Twenty-four hours later, the plates were placed in a radiofrequency field for 5 minutes at a generator power of 200 W (total generator power, 60 kJ). Forty-eight hours later, flow cytometry was performed. In a similar fashion, mixed cell populations ( $n = 4$ ) were also treated with conjugate concentrations of 30 nM for 3 hours and had a fresh media exchange, and the cells were exposed 24 hours later to a radiofrequency field for 4 minutes at 250 W (total generator power, 60 kJ).

### **Determination of Targeted Cells**

Transmission electron microscopy (TEM), fluorescence microscopy, and flow cytometry were used to discriminate between cocultured cells that contained cetuximab-conjugated nanoparticles and those that did not. TEM was performed with a JEM 1010 microscope (JEOL, Inc., Peabody, Mass), and images were taken with an AMT Imaging System (Advanced Microscopy Techniques Corp., Danvers, Mass). Fluorescence microscopy was performed with an Eclipse TE2000 microscope system (Nikon Instruments Inc., Melville, NY) with appropriate excitation and emission filters (Chroma Technology Corp., Rockingham, Vt).

### **Determination of Cell Death in the Context of Target Identification After Radiofrequency Therapy**

Cell populations were identified with flow cytometry that had high or low fluorescence of Qdot605, Qdot705, eFluor NC700, or Alexa Fluor 647 as an identifier (and in the case of quantum dots, the treatment). Cell death was determined by 7-amino-actinomycin D (BD Biosciences, Inc., San Jose, Calif). Annexin V, a well-characterized protein that binds to cellular inner membrane phospholipid phosphatidylserine exposed during apoptosis, was provided and conjugated to the fluorophore Horizon V450 as a kind gift from BD Biosciences.

### **Statistical Analysis**

Results are expressed as means  $\pm$  standard errors of the mean unless otherwise noted. Statistical significance,  $\alpha$ , was set to  $P < .05$ . Groups were compared with a 2-tailed Student *t*-test, unless otherwise noted. Data were analyzed

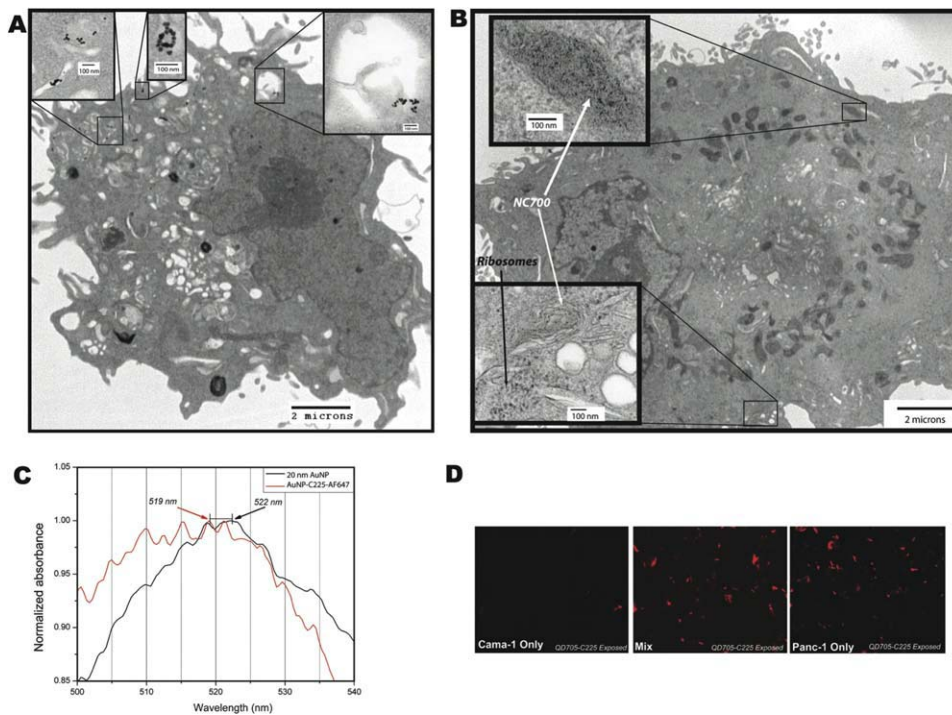


**Figure 1.** Cetuximab-conjugated nanoparticles are preferentially internalized into Panc-1 cells when observed by transmission electron microscopy: (A) gold nanoparticles (AuNP)-C225 and (B) eFluor NC700 (NC<sub>700</sub>)-C225. The figure bars represent 2  $\mu$ m, whereas the bars in the inset images represent 100 nm. Of note, the electron-dense cores of NC<sub>700</sub> quantum dots are smaller than ribosomes or gold nanoparticles. (C) A slight plasmon shift was noted when the antibody was conjugated to the gold nanoparticles. (D) Qdot705-C225 was observed predominately in Panc-1 cells of the fluorescence microscopy images (original magnification,  $\times 200$ ). The exposure time and settings for each fluorescence microscopic image were the same, whereas the red is false color.

and plotted with Microsoft Excel for Mac version 12 (Microsoft Corp., Redmond, Wash), SigmaPlot version 10 (Systat Software, Inc., San Jose, Calif), and FlowJo version 8.8.6 (Tree Star, Inc., Ashland, Ore).

## RESULTS

### *Production and Internalization of Gold Nanoparticles-C225*

After gold nanoparticles were conjugated to cetuximab-labeled Alexa Fluor 647 (C225-Alexa Fluor 647), there was a small plasmon resonance shift consistent with conjugation and not consistent with gold aggregation (Fig. 1). TEM demonstrated gold nanoparticles internalized into Panc-1 cells (Fig. 1) but not into Cama-1 cells.

### *Targeting and Identifying Quantum Dot-Containing Cells*

Panc-1 cells demonstrated increased uptake of C225-conjugated quantum dots by fluorescence microscopy, flow cytometry, and TEM (Fig. 1). The mixed Panc-1 and Cama-1 cocultured cells and Panc-1-only groups clearly

displayed fluorescence associated with Qdot705-C225, whereas the Cama-1-only group did not (Fig. 1, red false color). There was a 10- to 100-fold brighter intensity of quantum dot-containing cells compared with the negative population. This permitted discrimination between Panc-1 cells with internalized quantum dots or control cells not containing quantum dots.

### *Heating of Quantum Dots in a Radiofrequency Field*

Deionized water heats in a 200-W 13.56-MHz (8.0-kV/m) radiofrequency field at  $0.28^{\circ}\text{C}/\text{min} \pm 0.07^{\circ}\text{C}/\text{min}$ . One hundred nanomolar C225 antibody alone in deionized water heats at  $1.18^{\circ}\text{C}/\text{min} \pm 0.13^{\circ}\text{C}/\text{min}$  in the same field (Fig. 2). All 3 nanoparticle-C225 conjugates heated significantly faster, in a concentration-dependent fashion ( $P < .05$ , Fig. 2). One hundred nanomolar gold nanoparticle-C225 heated at  $17.4^{\circ}\text{C}/\text{min} \pm 1.2^{\circ}\text{C}/\text{min}$  ( $P < .006$  compared with C225 or deionized water alone). One hundred nanomolar Qdot705-C225 and 100 nM eFluor NC700-C225 heated at  $17.3^{\circ}\text{C}/\text{min} \pm 0.5^{\circ}\text{C}/\text{min}$  and  $8.7^{\circ}\text{C}/\text{min} \pm 0.2^{\circ}\text{C}/\text{min}$ , respectively (both

$P < .0005$  compared with C225 or deionized water alone). Because of the similar components in Qdot605, the Qdot605-C225 conjugate heated in a similar manner to Qdot705-C225.

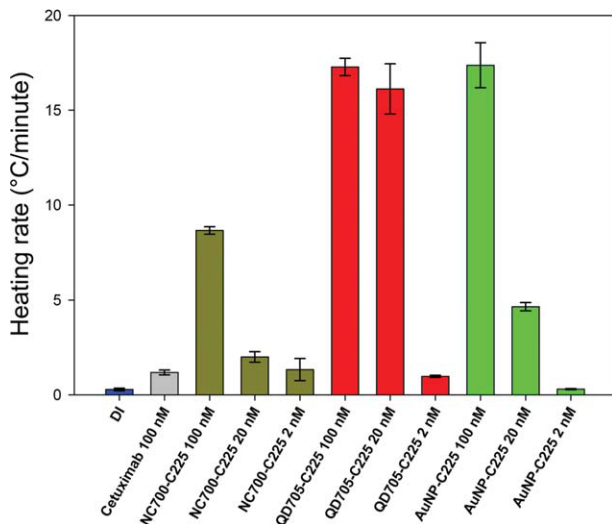


**Figure 2.** Solutions of cetuximab-conjugated gold nanoparticles (AuNP-C225) and quantum dots (NC<sub>700</sub>-C225 and Qdot705-C225) demonstrate a concentration-dependent heating rate. All solutions were diluted in 18 MΩ of water. Error bars are standard errors of the mean based on triplicate data for each conjugate. DI indicates deionized water.

### Radiofrequency Field-Induced Thermal Cytotoxicity in Panc-1 Cells

Control Panc-1 cells without quantum dots, gold nanoparticles, or radiofrequency treatment had a viability of  $99.0\% \pm 0.1\%$  (Fig. 3). After a 5-minute radiofrequency exposure without nanoparticles, the viability decreased to  $95.2\% \pm 2.2\%$ , as measured 48 hours after exposure. Treating Panc-1 cells with Qdot605-C225 conjugates without radiofrequency exposure decreased viability to  $82.2\% \pm 3.8\%$ . When Qdot605-C225-treated cells were subsequently placed in the radiofrequency field for 5 minutes, the viability decreased to  $47.5\% \pm 9.8\%$  ( $p \sim .0001$ ). Furthermore, radiofrequency field exposure of Qdot605-bearing Panc-1 cells induced cell necrosis, whereas Qdot605-C225 treatment without radiofrequency field exposure induced apoptotic cell death in a much smaller fraction of cells, as noted (Fig. 3). Qdot605-C225 was not used in the mixed cell experiments because it had heating characteristics similar to Qdot705-C225.

### Effects of Nanoparticle Treatment and Radiofrequency Field Exposure on Mixed Cell Populations

All subsequent studies with the remaining 3 nanoparticles conjugated to C225 (gold nanoparticles, Qdot705, eFluor NC700) were performed in Panc-1 and Cama-1 cells in

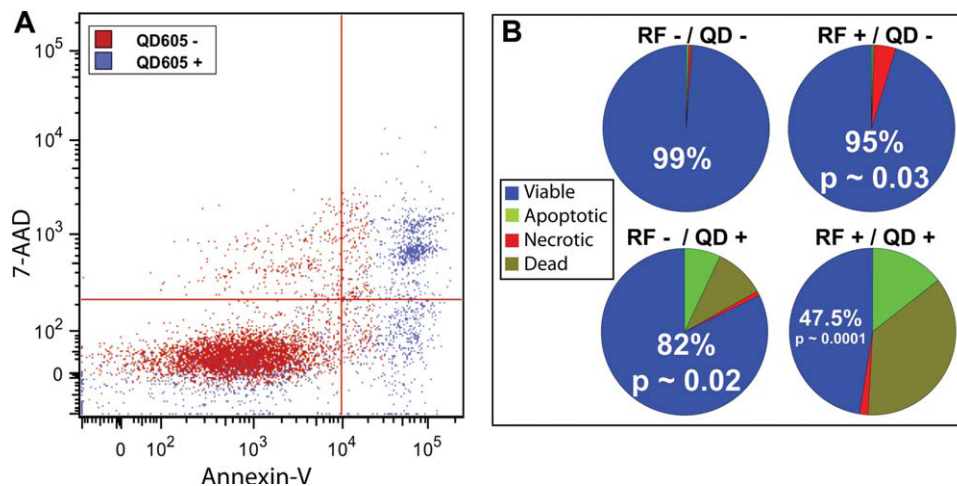


**Figure 3.** Panc-1 cells that were positive for quantum dot (QD<sub>605</sub>) fluorescence had significantly decreased viability compared with QD<sub>605</sub>-negative cells after radiofrequency (RF) field treatment ( $P = \sim .0001$ ). (A) On the flow cytometry live/dead plot, the lower left quadrant gates viable cells, the lower right quadrant gates apoptotic cells, the upper left quadrant gates necrotic cells, and the upper right quadrant gates dead cells of the single cell population. (B) The right panel summarizes the effects of treatment with QD<sub>605</sub>-C225 alone (RF-/QD+), the effects of radiofrequency exposure alone (RF+/QD-), and the combination (RF+/QD+) on the viability of Panc-1 cells as measured by flow cytometry compared with controls (RF-/QD-). The percentages in each pie chart represent the percentage viable, whereas the  $P$  values are compared with the RF-/QD- group. Before RF treatment, cells were treated with 50 nM QD<sub>605</sub>-C225 for 3 hours, whereas controls were treated with 50 nM C225 alone. Replicates are  $n = 4$ . 7-AAD indicates 7-amino-actinomycin D.

**Table 1.** Viability of Mixed Cell Populations After Treatment With 50 nM Cetuximab Conjugate and RF Field Exposure

Conjugate, 50 nM	RF Status	Viability $\pm$ SEM <sup>a</sup>	<i>P</i> <sup>b</sup>
NC <sub>700</sub> -C225	Cama-1 <sup>c</sup> RF-	96.5% $\pm$ 0.7%	—
	Cama-1 RF+	92.4% $\pm$ 2.58%	.2295
	Panc-1 <sup>d</sup> RF-	82.4% $\pm$ 1.9%	.0024
	Panc-1 RF+	58.2% $\pm$ 3.4%	.0004
QD <sub>705</sub> -C225	Cama-1 RF-	94.1% $\pm$ 0.5%	—
	Cama-1 RF+	92.8% $\pm$ 3.0%	.432
	Panc-1 RF-	73.7% $\pm$ 0.8%	<.0001
	Panc-1 RF+	56.3% $\pm$ 3.3%	<.0001
AuNP-C225	Cama-1 RF-	94.2% $\pm$ 2.0%	—
	Cama-1 RF+	93.7% $\pm$ 1.0%	.579
	Panc-1 RF-	86.3% $\pm$ 0.5%	.060
	Panc-1 RF+	39.4% $\pm$ 8.3%	.036

RF indicates radiofrequency; SEM, standard error of the mean; QD, quantum dots; AuNP, gold nanoparticles.

<sup>a</sup>SEM represents replicates of  $n = 4$ .

<sup>b</sup>Significance is compared to Cama-1 RF- within each group.

<sup>c</sup>Cama-1 cells have a minimal decrease in viability despite nanoparticle conjugate exposure and RF field treatment, due to the minimal internalization of nanoparticles related to the minimal expression of epidermal growth factor receptor-1.

<sup>d</sup>Panc-1 cells demonstrate decreased viability after treatment with a high concentration of cetuximab-conjugated nanoparticles (50 nM).

coculture. The relative positions of 2 individual populations of Cama-1 and Panc-1 cells on a side scatter Alexa Fluor 647 plot were used to identify 2 distinct cell populations in the experimental groups. A mixed cell population exposed to cetuximab-conjugated quantum dots displayed similar patterns for identification.

Cama-1 cells maintained viability  $>88\%$  after treatment with cetuximab-conjugated quantum dots and gold nanoparticles as measured 48 hours after radiofrequency field exposure (Table 1, Fig. 4). Low-dose treatment (30 nM) of all 3 cetuximab-nanoparticle conjugates decreased Panc-1 viability to an average of 78% after radiofrequency field exposure ( $P < .003$ ). Radiofrequency field treatment after 50 nM eFluor NC700-C225 yielded a Panc-1 cell viability rate of  $58.2\% \pm 3.4\%$ , whereas the viability rate was reduced to  $56.3\% \pm 3.3\%$  after 50 nM Qdot705-C225 treatment followed by radiofrequency field exposure (Table 1). Fifty nanomolar gold nanoparticles-C225-Alexa Fluor 647 treatment of mixed cell populations coupled with subsequent radiofrequency field exposure reduced Panc-1 viability to  $39.4\% \pm 8.3\%$  (Table 1,  $P \sim .036$ ). Qdot705-C225 and gold nanoparticles-C225 induced 3 to 4 $\times$  more necrosis than apoptosis in Panc-1 cells after radiofrequency exposure ( $P \sim .01$  for Qdot705-C225 and  $P \sim .003$  for gold nanoparticles-C225), whereas eFluor NC700-C225 induced twice as much apoptosis as necrosis after radiofrequency exposure in Panc-

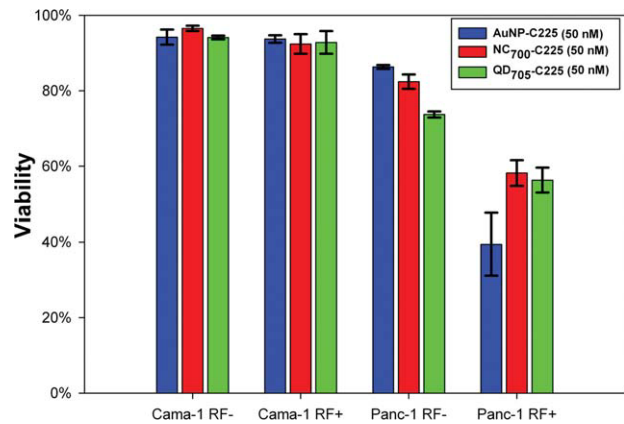


**Figure 4.** The viability of Panc-1 cells, but not Cama-1 cells, decreases after treatment with cetuximab conjugates (50 nM) and radiofrequency (RF) field exposure (200 W for 5 minutes.). Cell death is most clearly demonstrated for gold nanoparticles (AuNP) targeted to Panc-1 cells after RF field exposure. RF field exposure after treatment with quantum dots (QD<sub>705</sub>-C225 and NC<sub>700</sub>-C225) was also sufficient to produce significant cytotoxicity compared with Cama-1 cells that did not take up the targeted nanoparticles.

1 cells ( $P \sim .017$ , Table 2). Cama-1 cell viability after radiofrequency field exposure was  $93.7\% \pm 1.0\%$ ,  $92.8\% \pm 3.0\%$ , and  $92.4\% \pm 2.6\%$ , respectively, after treatment with 50 nM gold nanoparticles-C225-Alexa Fluor 647, Qdot705-C225, and eFluor NC700-C225 (Table 1).

## DISCUSSION

In this model, a noninvasive, nonionizing shortwave radiofrequency field induced a concentration-dependent cytotoxicity in malignant human cells first treated with antibody-targeted nanoparticles. We demonstrated that the cell-specific intracellular hyperthermia caused minimal toxicity to bystander cells that did not take up the EGFR-targeted nanoparticles. Interestingly, the gold nanoparticles-C225-Alexa Fluor 647 treatment induced the greatest cell death after a single radiofrequency field exposure. We suggest that intense heat release during radiofrequency field exposure in the nanoscale environment immediately around each nanoparticle dominates the cellular killing effect through protein denaturation and disruption of cellular membranes.<sup>25</sup> Measuring bulk temperatures only approximates the heat transfer from the nanoparticle to the surrounding intracellular environment. At the intracellular level, most likely a relatively low concentration of nanoparticles will be sufficient to induce irreparable injury if structures requisite for cell viability (ie, nucleus, mitochondria, intact cell membrane) are severely damaged or destroyed. This is consistent with the

**Table 2.** Distribution of Viability After Treatment With 50 nM Cetuximab Conjugates and RF Field Exposure<sup>a</sup>

Conjugate, 50 nM	Necrotic, (% ± SEM) <sup>b</sup>	Dead (% ± SEM)	Apoptotic (% ± SEM)	Viable (% ± SEM)
<b>NC<sub>700</sub>-C225</b>				
Cama-1	1.88 ± 0.73	3.41 ± 1.00	2.29 ± 1.04	92.40 ± 2.78
Panc-1	6.62 ± 0.89	21.50 ± 1.05	13.70 ± 1.98	58.20 ± 3.41
<b>QD<sub>705</sub>-C225</b>				
Cama-1	2.39 ± 0.36	0.82 ± 0.24	4.06 ± 1.05	92.80 ± 1.09
Panc-1	26.50 ± 5.06	9.94 ± 2.20	7.27 ± 1.56	56.30 ± 3.27
<b>AuNP-C225</b>				
Cama-1	1.46 ± 0.43	0.70 ± 0.16	4.08 ± 1.05	93.73 ± 1.04
Panc-1	33.23 ± 3.95	18.75 ± 4.20	8.68 ± 3.07	39.35 ± 8.24

RF indicates radiofrequency; SEM, standard error of the mean; QD, quantum dots; AuNP, gold nanoparticles.

<sup>a</sup>Cetuximab-conjugated nanoparticles induce both apoptosis and necrosis of targeted cells (Panc-1) after treatment in an RF field. This table displays the distribution of necrosis, apoptosis, and dead and viable cells of the single cell population after exposure to 50 nM of cetuximab conjugates and RF field treatment (200 W for 5 minutes.).

<sup>b</sup>SEM represent replicates of  $n = 4$ .

interesting finding that Qdot705-C225 and gold nanoparticles-C225 not only heat much faster than eFluor NC700-C225, but they also induce a predominately necrotic radiofrequency-induced effect, whereas the eFluor NC700-C225 conjugates were associated with lower rates of radiofrequency-induced heating that predominately induced apoptosis (Table 2). As we have demonstrated, nuances regarding the magnitude of intracellular hyperthermia (media temperatures remained  $<40.5^{\circ}\text{C}$  at all times here) seem to determine whether cellular death is via apoptotic or necrotic pathways in general.

Although all of the nanoparticles presented here have a hydrodynamic diameter of  $\sim 20$  nm,<sup>20,21</sup> the surface area of the solid gold nanoparticles has more exposure to the radiofrequency field per particle, because they are larger than the core of the quantum dots. Although larger semiconducting nanocrystals will fluoresce in the very far red to near infrared region, the semiconducting nature of the particles may permit increased heat dissipation at larger diameters, whereas gold nanoparticles tend to heat less when they are greater than  $\sim 50$  nm in diameter.<sup>7</sup> In addition, as the underlying theory requires transfer of energy to the surrounding intracellular milieu, different coatings among different nanoparticles may abrogate or enhance the radiofrequency field-induced heating. Surface coatings and functionalizing molecules are variable from nanoparticle to nanoparticle and often synthesis dependent.

The heating rates reported here are not extremely high ( $<20^{\circ}\text{C}/\text{min}$ ) because of the low generator powers. This was intentional, to prevent any nonspecific heating of the media to temperatures  $>40.5^{\circ}\text{C}$ . Although prolonged exposure times are required for cell death between

$40.5^{\circ}\text{C}$  and  $43^{\circ}\text{C}$ , apoptosis begins at these temperatures.<sup>4</sup> However, as has been demonstrated here, quantum dots or gold nanoparticles internalized into cancer cells do in fact produce sufficient intracellular hyperthermia in response to the shortwave radiofrequency field exposure to induce significant cell death after a single treatment.

The cytotoxicity of quantum dots is being investigated, with some types having more potential toxic effects than others.<sup>12,26-28</sup> Qdot605 and Qdot705, for example, contain a well-known cytotoxic agent, cadmium. Although the toxicity associated with free cadmium ions varies with the specific quantum dot and cell under investigation, quantum dot toxicity has been reported at concentrations  $>0.8$   $\mu\text{M}$ .<sup>26</sup> In general, in vitro models suggest that cadmium quantum dot concentrations  $<100$  nM are safely tolerated, and indium-based quantum dots (ie, eFluor NC700) are  $10\times$  less toxic.<sup>22,28,29</sup> Although certain metals (ie, platinum) have become standard treatment for some cancers,<sup>30</sup> cadmium toxicities to normal cells makes cadmium an unattractive option as an anti-cancer cytotoxic agent. Unfortunately, each type of quantum dot is unique, with its own toxicity profile. The type of core, shell, and coating all contribute to variations in release of free ions that may induce cytotoxicity.<sup>22</sup>

The ideal theranostic agent would not only permit diagnosis and treatment of cancer cells, but also permit multimodality treatment without injury to bystander cells. Although multiple agents can be conjugated to a single nanoparticle, the use of quantum dots permits 1 less conjugation because of the bifunctionality of fluorescence and local nanoscale hyperthermia in a radiofrequency field. This is a potentially important new finding and an addition to the multifunctionality of quantum dots,

nanocrystals, or other fluorescent nanoparticles. These types of nanoparticles have already been used for in vitro and in vivo optical imaging in animal models of malignant cells, including breast, prostate, and pancreatic cancer.<sup>31-33</sup> Including other elements in the core or shell structure, such as iron, gadolinium, or gold, may allow the nanoparticles to be used for optical and radiographic imaging with magnetic resonance or computed tomographic scans.<sup>33</sup> Some fluorescent nanoparticles can bind to specific proteins, creating the potential to measure circulating serum or intracellular protein levels.<sup>34</sup> Plasmon-coupling can be used to observe specific base pair mismatches or mutations in DNA using thiolated DNA probes linked to gold nanoparticles because of specific surface-enhanced Raman scattering.<sup>35</sup> Functionalization and enhancement of circulating half-life of fluorescent nanoparticles can be achieved by linking PEG, proteins, silica, or other biocompatible polymers to the fluorescent core.<sup>31,33,36</sup> Targeting molecules, including antibodies, peptides, or pharmacologic agents, can also be arrayed on the surface to promote cell-specific binding and uptake. This may permit targeted delivery of drugs, silencing RNA, or other therapeutic agents to malignant cells with successful delivery confirmed by noninvasive optical imaging. We have shown in this study that the intrinsic fluorescence of quantum dots and nanocrystals is useful in flow cytometric analysis and identification of specific cell populations. Heat release during radiofrequency field exposure in these semiconducting quantum dots and nanocrystals has not previously been reported, and this opens yet another potential therapeutic use for fluorescence nanoparticles. Cetuximab is an excellent antibody for in vitro models because of the variation in EGFR-1 expression of different cancer cell lines; however, it would be a poor choice in human trials, as EGFR-1 is constitutively expressed in many normal tissues, but overexpressed in a minority of cancers.<sup>37</sup> A major challenge in cancer therapy is to identify cellular targets that are uniquely expressed only on malignant cells. This goal has yet to be fully realized. However, as antibody, drug, and peptide binding to cancer-specific targets identified through genetic and proteomic analyses<sup>38,39</sup> becomes more specific, using bifunctional fluorescent nanoparticles may permit diagnostic and treatment options that are noninvasive and minimally toxic.

#### CONFLICT OF INTEREST DISCLOSURES

Support from an unrestricted research grant was provided by the Kanzius Research Foundation (Erie, Pa). In addition, Dr. Glazer

was supported as a T32 research fellow funded by the National Cancer Institute at the National Institutes of Health (5 T32 CA09599). The Cell Line Characterization Core and High Resolution Transmission Electron Microscopy Core are funded by National Cancer Institute, grant CA16672.

#### REFERENCES

1. Kam NW, O'Connell M, Wisdom JA, Dai H. Carbon nanotubes as multifunctional biological transporters and near-infrared agents for selective cancer cell destruction. *Proc Natl Acad Sci U S A*. 2005;102:11600-11605.
2. El-Sayed IH, Huang X, El-Sayed MA. Selective laser photothermal therapy of epithelial carcinoma using anti-EGFR antibody conjugated gold nanoparticles. *Cancer Lett*. 2006;239:129-135.
3. Huang X, El-Sayed IH, Qian W, El-Sayed MA. Cancer cell imaging and photothermal therapy in the near-infrared region by using gold nanorods. *J Am Chem Soc*. 2006;128:2115-2120.
4. Tell RA, Harlen F. A review of selected biological effects and dosimetric data useful for development of radiofrequency safety standards for human exposure. *J Microw Power*. 1979;14:405-424.
5. Curley SA, Cherukuri P, Briggs K, et al. Noninvasive radiofrequency field-induced hyperthermic cytotoxicity in human cancer cells using cetuximab-targeted gold nanoparticles. *J Exp Ther Oncol*. 2008;7:313-326.
6. Gannon CJ, Cherukuri P, Jakobson BI, et al. Carbon nanotube-enhanced thermal destruction of cancer cells in a noninvasive radiofrequency field. *Cancer*. 2007;110:2654-2665.
7. Moran CH, Wainderdi SM, Cherukuri TK, et al. Size-dependent joule heating of gold nanoparticles using capacitively coupled radiofrequency fields. *Nano Res*. 2009;2:400-405.
8. Sumer B, Gao JM. Theranostic nanomedicine for cancer. *Nanomedicine*. 2008;3:137-140.
9. Mattoussi H, Mauro JM, Goldman ER, et al. Bioconjugation of highly luminescent colloidal CdSe-ZnS quantum dots with an engineered 2-domain recombinant protein. *Physica Status Solidi B Basic Res*. 2001;224:277-283.
10. Medintz IL, Uyeda HT, Goldman ER, Mattoussi H. Quantum dot bioconjugates for imaging, labelling and sensing. *Nat Materials*. 2005;4:435-446.
11. Meng L, Song ZX. Applications of quantum dots to biological medicine. *Prog Biochem Biophys*. 2004;31:185-187.
12. Walling MA, Novak JA, Shepard JRE. Quantum dots for live cell and in vivo imaging. *Int J Mol Sci*. 2009;10:441-491.
13. Dabbousi BO, Rodriguez Viejio J, Mikulec FV, et al. (CdSe)ZnS core-shell quantum dots: synthesis and characterization of a size series of highly luminescent nanocrystals. *J Phys Chem B*. 1997;101:9463-9475.
14. Green M. Solution routes to III-V semiconductor quantum dots. *Curr Opin Solid State Materials Sci*. 2002;6:355-363.
15. Parak WJ, Pellegrino T, Plank C. Labelling of cells with quantum dots. *Nanotechnology*. 2005;16:R9-R25.
16. Gao X, Dave SR. Quantum dots for cancer molecular imaging. *Adv Exp Med Biol*. 2007;620:57-73.
17. Kairdolf BA, Mancini MC, Smith AM, Nie S. Minimizing nonspecific cellular binding of quantum dots with hydroxyl-derivatized surface coatings. *Anal Chem*. 2008;80:3029-3034.

18. Mancini MC, Kairdolf BA, Smith AM, Nie S. Oxidative quenching and degradation of polymer-encapsulated quantum dots: new insights into the long-term fate and toxicity of nanocrystals in vivo. *J Am Chem Soc.* 2008;130:10836-10837.
19. Michalet X, Pinaud FF, Bentolila LA, et al. Quantum dots for live cells, in vivo imaging, and diagnostics. *Science.* 2005;307:538-544.
20. Yildiz I, McCaughan B, Cruickshank SF, Callan JF, Raymo FM. Biocompatible CdSe-ZnS core-shell quantum dots coated with hydrophilic polythiols. *Langmuir.* 2009;25:7090-7096.
21. Liu W, Howarth M, Greytak AB, et al. Compact biocompatible quantum dots functionalized for cellular imaging. *J Am Chem Soc.* 2008;130:1274-1284.
22. Derfus AM, Chan WCW, Bhatia SN. Probing the cytotoxicity of semiconductor quantum dots. *Nano Lett.* 2004;4:11-18.
23. Patra CR, Bhattacharya R, Wang E, et al. Targeted delivery of gemcitabine to pancreatic adenocarcinoma using cetuximab as a targeting agent. *Cancer Res.* 2008;68:1970-1978.
24. Wishart DS, Knox C, Guo AC, et al. DrugBank: a knowledgebase for drugs, drug actions and drug targets. *Nucleic Acids Res.* 2008;36:D901-D906.
25. Gannon CJ, Patra CR, Bhattacharya R, Mukherjee P, Curley SA. Intracellular gold nanoparticles enhance non-invasive radiofrequency thermal destruction of human gastrointestinal cancer cells. *J Nanobiotechnol.* 2008;6:2.
26. Kirchner C, Liedl T, Kudera S, et al. Cytotoxicity of colloidal CdSe and CdSe/ZnS nanoparticles. *Nano Lett.* 2005;5:331-338.
27. Chang YP, Pinaud F, Antelman J, Weiss S. Tracking biomolecules in live cells using quantum dots. *J Biophotonics.* 2008;1:287-298.
28. Hardman R. A toxicologic review of quantum dots: toxicity depends on physicochemical and environmental factors. *Environ Health Perspect.* 2006;114:165-172.
29. Male KB, Lachance B, Hrapovic S, Sunahara G, Luong JHT. Assessment of cytotoxicity of quantum dots and gold nanoparticles using cell-based impedance spectroscopy. *Anal Chem.* 2008;80:5487-5493.
30. Wang D, Lippard SJ. Cellular processing of platinum anticancer drugs. *Nat Rev Drug Discov.* 2005;4:307-320.
31. Yang L, Mao H, Cao Z, et al. Molecular imaging of pancreatic cancer in an animal model using targeted multifunctional nanoparticles. *Gastroenterology.* 2009;136:1514.e2-1525e2.
32. Zhang J, Su J, Liu L, Huang Y, Mason RP. Evaluation of red CdTe and near infrared CdHgTe quantum dots by fluorescent imaging. *J Nanosci Nanotechnol.* 2008;8:1155-1159.
33. Sajja HK, East MP, Mao H, Wang YA, Nie S, Yang L. Development of multifunctional nanoparticles for targeted drug delivery and noninvasive imaging of therapeutic effect. *Curr Drug Discov Technol.* 2009;6:43-51.
34. Mei F, He XW, Li WY, Zhang YK. Preparation and characterization of CdHgTe nanoparticles and their application on the determination of proteins. *J Fluoresc.* 2008;18:883-890.
35. Qian X, Zhou X, Nie S. Surface-enhanced Raman nanoparticle beacons based on bioconjugated gold nanocrystals and long range plasmonic coupling. *J Am Chem Soc.* 2008;130:14934-14935.
36. Wolcott A, Gerion D, Visconte M, et al. Silica-coated CdTe quantum dots functionalized with thiols for bioconjugation to IgG proteins. *J Phys Chem B.* 2006;110:5779-5789.
37. Herbst RS, Shin DM. Monoclonal antibodies to target epidermal growth factor receptor-positive tumors: a new paradigm for cancer therapy. *Cancer.* 2002;94:1593-1611.
38. Tonon G. From oncogene to network addiction: the new frontier of cancer genomics and therapeutics. *Future Oncol.* 2008;4:569-577.
39. Schrattenholz A, Soskic V. What does systems biology mean for drug development? *Curr Med Chem.* 2008;15:1520-1528.